Tone Generation by Rotor-Downstream Strut Interaction

Richard P. Woodward* and Joseph R. Balombin†
NASA Lewis Research Center, Cleveland, Ohio

A JT15D fan stage was acoustically tested in the NASA Lewis anechoic chamber as part of the joint Lewis/Langley Research Center investigation of flight simulation techniques and flight effects using the JT15D engine as a common test vehicle. Suspected rotor-downstream support strut interaction was confirmed through the use of simulated support struts, which were tested at three axial rotor-strut spacings. Tests were also performed with the struts removed. Inlet boundary layer suction in conjunction with an inflow control device was also explored. The removal of the boundary layer reduced the fan fundamental tone levels, suggesting that the mounting and mating of such a device to the nacelle requires careful attention. With the same inflow control device installed, good acoustic agreement was shown between the engine on an outdoor test stand and the fan in the anechoic chamber.

Introduction

THE development of effective inflow control devices (ICD's) makes it possible to study noise generation mechanisms, such as rotor-stator interaction, with reduced masking effects of inflow disturbances. Modern turbofan engines are often designed with blade/vane numbers selected to prevent propagation of the fundamental rotor-stator interaction tone. However, less consideration has been given to possible rotor interactions with engine support struts. These struts are either located downstream of the stator row or are integrated into the stator as large cross-section vanes.[1]

This paper presents results for a JT15D fan stage which was acoustically tested in the NASA Lewis Research Center anechoic chamber[2] as part of a joint NASA Lewis/Langley investigation of flight simulation techniques and flight effects using the JT15D-1 engine as a common test vehicle.[3-7] The engines used in these studies were instrumented with blade and vane pressure transducers to assist in isolating noise generation mechanisms. Although the primary goal of this study was to evaluate inflow control techniques, the results revealed that for the JT15D-1 engine in particular speed ranges the fundamental tone was controlled by the presence of six engine support struts located downstream of the stator. Blade pressure results showing a strong six per revolution disturbance pointed to these struts as the probable noise source. The interaction between the 28-blade rotor of the JT15D and the six support struts would result in a $m=22$ acoustic spinning mode having 22 circumferential lobes. This mode was shown to exist in the inlet duct of a JT15D engine when the results from two pressure sensors located in the duct so as to allow spining mode identification by signal phase relationship were used.[3] However, it was not possible to alter the support struts in the engine to establish the behavior of this apparent noise source.

Downstream support struts were not required for the JT15D fan installation in the anechoic chamber. Six simulated support struts were fabricated and installed in the test fan stage to simulate the actual engine support strut installation. These simulated struts were located at three axial spacings from the stator trailing edge. Thus, in the present study results were obtained for the spacing effect of downstream support struts as well as for fan stage alone with no downstream struts.

Received April 22, 1983; revision received Sept. 16, 1983.

*Aerospace Engineer. Member AIAA.
†Aerospace Engineer.

Two possible mechanisms could produce rotor-strut noise: the rotor wake could impinge on the struts, or the strut potential field could extend upstream to influence the rotor. Results from Ref. 8 suggest that this second mechanism may be the case. In this reference, tests with a two-stage fan with downstream struts showed that the potential field of these struts could induce significant blade vibration in the upstream rotor. In fact, the data analysis in this reference suggests that the strut potential field is transmitted through the stator row with little loss in magnitude, resulting in an effective closer rotor-strut spacing.

The inflow control study of the JT15D fan stage in the anechoic chamber made use of two inflow control devices which were previously tested at Lewis on the JT15D-1 engine.[3,7] In addition, the anechoic chamber installation had provisions for inlet boundary layer suction. The fan stage could be run with either a hard inlet duct surface or with a porous metal section in the outer duct wall, which was connected to a suction system to allow removal of about 10% of the inlet airflow. Removing the boundary layer could possibly eliminate irregularities contained in streamlines near the wall before they reached the rotor, thus reducing this possible noise source. The inlet was run with hard walls except for the boundary layer suction tests. Results for another fan tested in an anechoic chamber suggested that boundary layer suction may lower the fan blade passage tone level through the removal of such flow irregularities.[9]

Apparatus and Procedure

Anechoic Chamber

Figure 1 is a photograph of the Lewis anechoic chamber. The research fan shown in the chamber does not have an inflow control device installed. Also seen in this photograph are some of the fixed-position microphones and the traversing boom microphone. Calibration of the chamber showed it to be anechoic to within 2 dB for frequencies above 200 Hz.

Research Fan

The JT15D fan stage was installed in the anechoic chamber with an ICD attached to the inlet as shown in Fig. 2. The fan stage used the same bypass flow passage contours as did the actual JT15D-1 engine. The core drive of the engine was replaced by an external electric drive, with the fan airflow exhausting through a collector assembly. Table 1 presents selected fan stage design parameters. The production JT15D-1 engine had 33 core stator vanes. For acoustic cutoff considerations, an aerodynamically similar 71-vane core stator was used for this acoustic program. Simulated engine support struts could be installed in the fan bypass duct as shown in

Table 1 Fan stage parameters at takeoff thrust for JT15D-1 engine

Rotor blades	28
Bypass stator vanes	66
Core stator vanes[a]	71
Speed, rpm	15,740
Rotor diameter, cm	53
Bypass ratio	3.3
Bypass pressure ratio	1.5
Total mass flow, kg/sec	34.5
Bypass mass flow, kg/sec	26.3
Bypass rotor-stator spacing	1.83 projected axial
Core rotor-stator spacing	1.42 rotor chords
Rotor-bypass strut spacing	4.92 (5.1 cm)

[a]Modified from production engine.

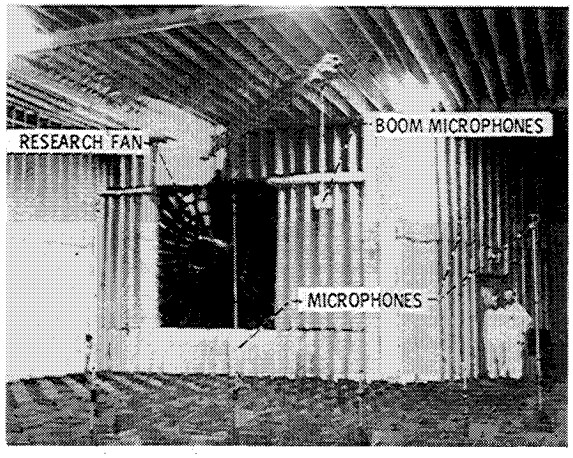

Fig. 1 Research fan installed in anechoic chamber.

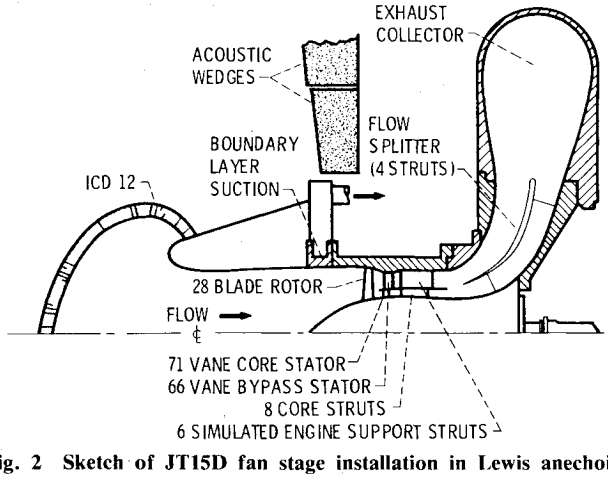

Fig. 2 Sketch of JT15D fan stage installation in Lewis anechoic chamber.

Fig. 3 at axial spacings of 2.5, 5.1 (engine design spacing), and 8.9 cm from the stator trailing edge. These struts had an axial length of 14.5 cm. The fan installation also had eight thin sheet metal turning vanes located in the core flow passage to straighten to axial the 25-deg flow swirl exiting the core stator. These thin cross-section vanes were not expected to affect the fan acoustic performance.

The boundary-layer suction assembly shown in Fig. 2 allowed removal of a portion of the inlet flow near the outer wall to reduce flow irregularities in this region and hence reduce this possible noise source. Outer wall airflow was removed through a 5.4 cm (2.5 in.) length of porous treatment located 15.2 cm (6 in.) upstream of the rotor face. The inlet was run with hard walls except for the boundary-layer suction tests.

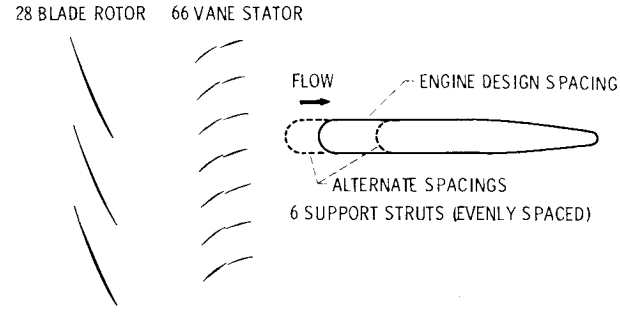

Fig. 3 Unwrapped bypass outside diameter flow passage of the JT15D fan stage, showing spacings for the simulated engine support struts.

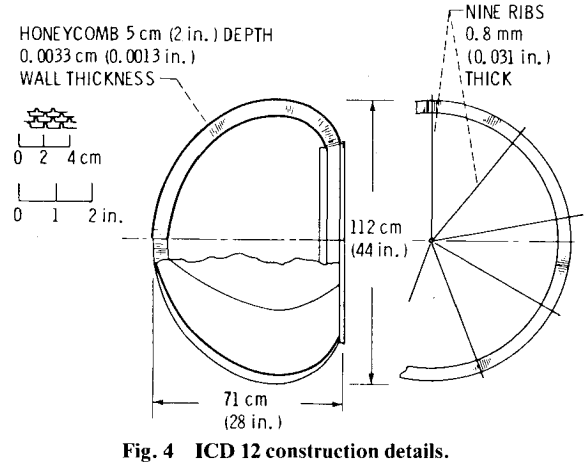

Fig. 4 ICD 12 construction details.

Figure 2 shows the fan stage installed in the anechoic chamber with inflow control device No. 12 attached in the fan inlet. Construction details of this ICD are shown in Fig. 4. This ICD was shaped so that the honeycomb cells are aligned with the flow streamlines calculated from a potential flow program. A second ICD, designated No. 5, was dimensionally similar, except that it had six, rather than nine, support ribs, an inner support wire mesh, and mounted on the fan inlet slightly ahead of where ICD 12 mounted. Further construction details of ICD 12 may be found in Ref. 7; details of ICD 5 are in Ref. 3. Except where noted, all results in this paper are for ICD 12.

Dynamic Instrumentation Data Reduction

In this test program, both rotor and stator were instrumented with high response pressure transducers.[10] Signals from the stator were brought out directly, while those from the rotor were FM transmitted from an antenna mounted in the spinner to another mounted along the inside casing. Results for the B3 transducer, which was located near the rotor tip (Fig. 5), are presented in this paper. Installation of these small devices (1.2 mm diameter sensing area, 0.8 mm thickness) involved cementing them to shims at the blade surface, and then fairing over them.

Data reduction of the pressure signals consisted primarily of computing the average pressure over a revolution and the corresponding spectra. Spectra were computed with a nominal 20 Hz resolution for 512 revolutions of the fan. A tachometer pulse occurring once per revolution was used to synchronize these analyses with the fan speed so that pressure variations not synchronized to the fan speed would be discounted.

Acoustic Instrumentation

Far field acoustic data were acquired on a 7.6 m radius from 0 to 90 deg from the fan inlet axis in 10-deg increments. Signals from the 0.64 cm (0.25 in.) diameter microphones

were recorded on magnetic tape for later narrow bandwidth spectral analysis. The output of this narrow bandwidth sound pressure level analysis was digitized and transmitted to a computer for further analysis. Using a computer reduction program, narrow bandwidth sound power level spectra were generated for the forward hemisphere (0 to 90 deg from the fan inlet axis). These spectra were averaged over 20 seconds, generally resulting in an uncertainty of less than 1 dB.

The boom microphone (seen in Fig. 2) was used to obtain continuous directivity results at a 6.1 m radius centered in the plane of the fan inlet highlight. A narrow bandwidth spectral analyzer was used to determine the fundamental and overtone levels for these boom traverses.

Results and Discussion

Aerodynamic Results

The fan operating map (Fig. 6) shows the aerodynamic performance of the JT15D fan as tested in the anechoic chamber. The flow restrictions in the exhaust ducts were adjusted for fan operation on the same operating line as that measured for the JT15D-1 engine at the Lewis vertical lift facility (VLF). Overlaid results from the statically tested VLF engine tests show good agreement with the fan results.

Support Strut Effect

Since engine support struts are not needed in this anechoic chamber fan installation, an opportunity was available to perform tests both without struts and with simulated struts to better understand the apparent rotor-strut interaction observed in the engine tests. Simulated engine support struts were installed in the downstream bypass flow passage at three axial rotor-strut spacings as shown in Fig. 3.

Far Field Acoustic Effects

Figure 7 shows how the sound power level (0 to 90 deg from the fan inlet axis) at the blade passage tone (BPT) changes

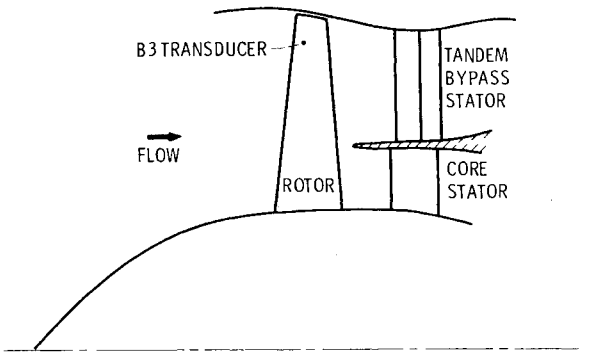

Fig. 5 Location of B3 pressure transducer (pressure side of blade, 0.38 cm from blade leading edge, 1.90 cm from tip).

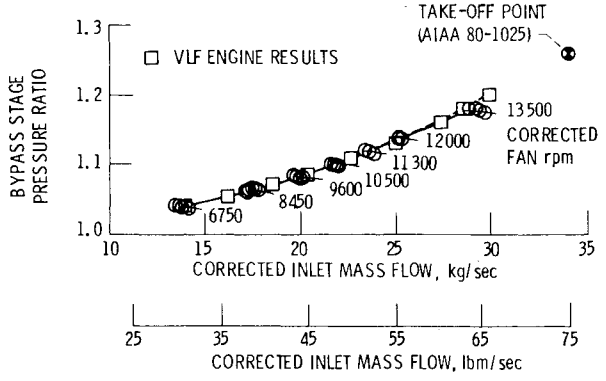

Fig. 6 Fan operating map (VLF engine results shown for comparison).

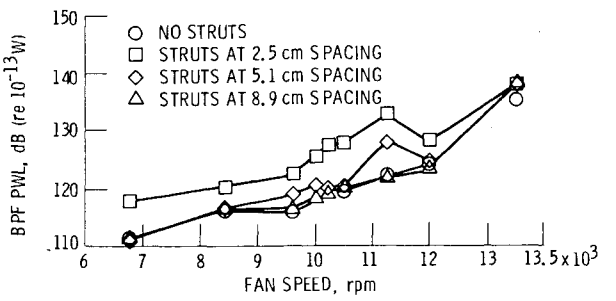

Fig. 7 Strut spacing effect on fundamental blade passage tone power as a function of fan speed (0-90 deg, 80 Hz bandwidth).

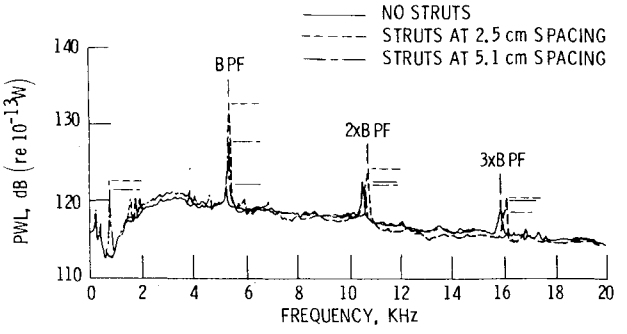

Fig. 8 Sound power level spectra as a function of strut location (0-90 deg, 11, 300 rpm, 80 Hz bandwidth)

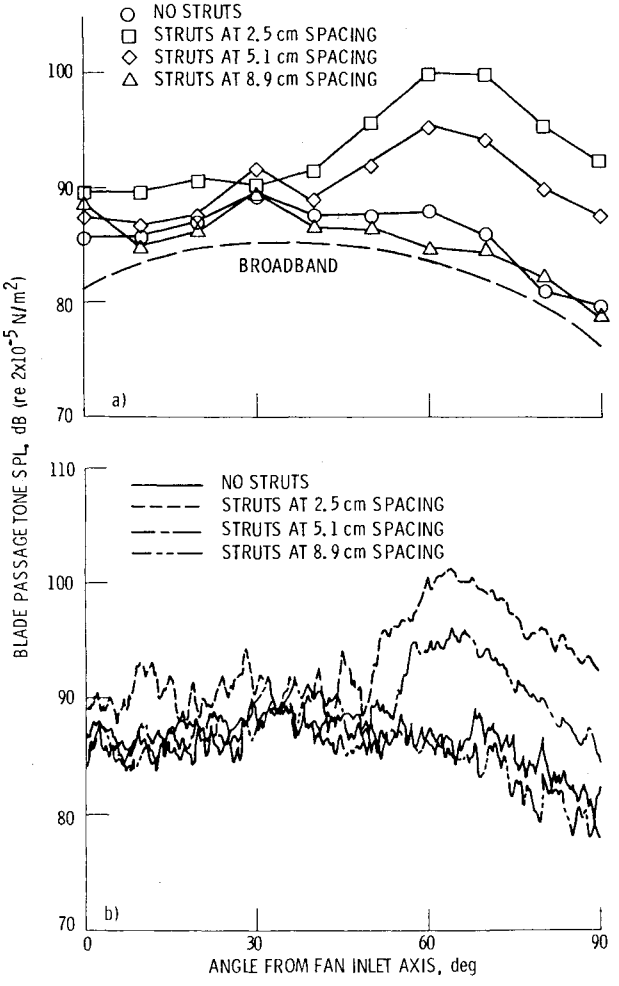

Fig. 9 Strut spacing effect on blade passage tone directivity (11,300 rpm); a) fixed-position microphones, b) boom microphone.

with fan speed for the three strut positions and also for no struts. The struts clearly increase the tone level at the 2.5 and 5.1 cm spacings. The closest spacing results in an increase of the tone level of 10 dB at 11, 300 rpm fan speed. With the struts at the engine design spacing of 5.1 cm, there is still a significant strut-induced tone, with the greatest effect seen for fan operation at 11, 300 rpm. There was no significant strut effect on sound power of this BPT at the 8.9 cm spacing.

The sound power level spectra for no struts and for the struts at the two closer spacings are shown in Fig. 8 at 11, 300 rpm. Again the strong effect of strut location on the fundamental tone can be seen. The presence of the struts has little influence on the overtone ($2\times$BPF and $3\times$BPF) or on broadband noise levels. The spectral spike located at about 800 Hz is seen only when the struts are in place. This spike is most probably the Strouhal shedding tone from the struts, which occurs at about 850 Hz for this fan speed.

The blade passage tone directivities for the three strut spacings and for no struts are presented in Fig. 9 at 11, 300 rpm. The results for the fixed-position microphone are shown in Fig. 9b. There is excellent agreement between the results of Fig. 9a and 9b, with the boom microphone results providing an improved resolution of the directivity. The presence of the struts at the two closer spacings clearly has an effect on the directivity, resulting in a distinct lobe peaking in the range from 60 to 70 deg. This is the 22-lobe mode identified in Ref. 3. At the widest strut spacing the sound pressure level and directivity were essentially the same as for the no-strut case.

The distinctive directivity pattern of the close strut spacings is primarily due to the 22-lobe pattern identified in Ref. 3 and discussed in the Introduction. Other circumferential modes, such as $m=16$ and 10 are possible, due to rotor interaction with higher harmonics of strut-induced distortion.

The cut-off ratio[11] ξ is a basic parameter for determining mode propagation, where ξ must be greater than 1.0 for the mode to be observed in the far field. This parameter is defined as:

$$\xi = \left|\frac{nB}{m}\right| M_T/M^*_{mn}\sqrt{1-M_D^2} \qquad (1)$$

where

B = rotor blade number
V = stator (or strut) vane number
M_T = equivalent rotor tangential Mach number at a particular wall radius
M_D = duct Mach number (negative value for inlet flow into fan)
m = $nB-kV$, mode circumferential lobe number
n = harmonic number (1 for BPF, 2 for $2\times$BPF, etc.)
k = integer
M^*_{mn} = mode eigenvalue/m

It is assumed that there is a location between the inlet throat and highlight at which the wall no longer influences inlet radiation and that the inlet diameter at this location should be used for calculating M_T in Eq. (1). However, the location where "acoustic separation" occurs is not yet known from theory, and it also should depend on the particular mode present. Thus, in the absence of a detailed analysis to determine M_T, the cutoff ratio values based on the throat and highlight diameters will be considered in the directivity calculations which follow to bracket the possible ranges.

The theoretical directivity models for mode propagation developed in Refs. 11 and 12 may be compared to the results of the present study. In static tests, the angle where the principal lobe of the acoustic spinning mode is expected to have a maximum value is expressed as[12]

$$\cos\psi_\chi = \left(M_D+\sqrt{1-1/\xi^2}\right)\Big/\left(1+M_D\sqrt{1-1/\xi^2}\right) \qquad (2)$$

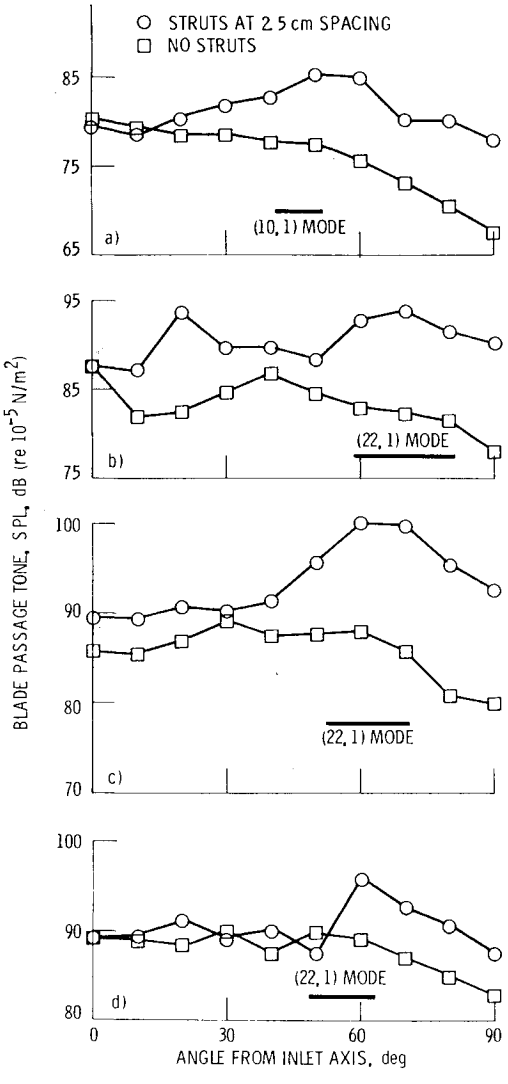

Fig. 10 Blade passage tone directivity at several fan speeds; a) 6750 rpm, b) 10,500 rpm, c) 11,300 rpm, d) 12,000 rpm.

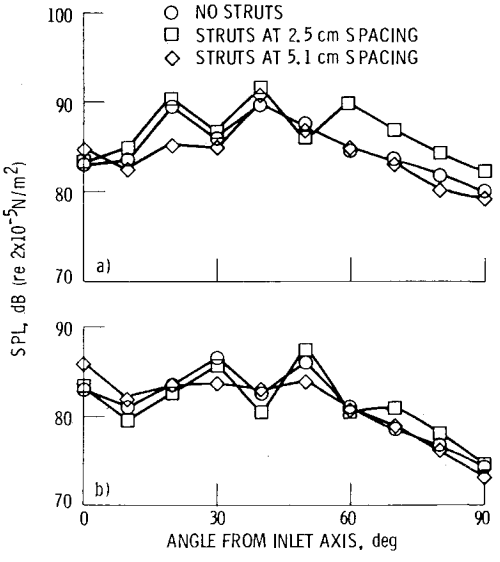

Fig. 11 Strut spacing effect on first and second overtone directivity (11,300 rpm); a) $2\times$BPF, b) $3\times$BPF.

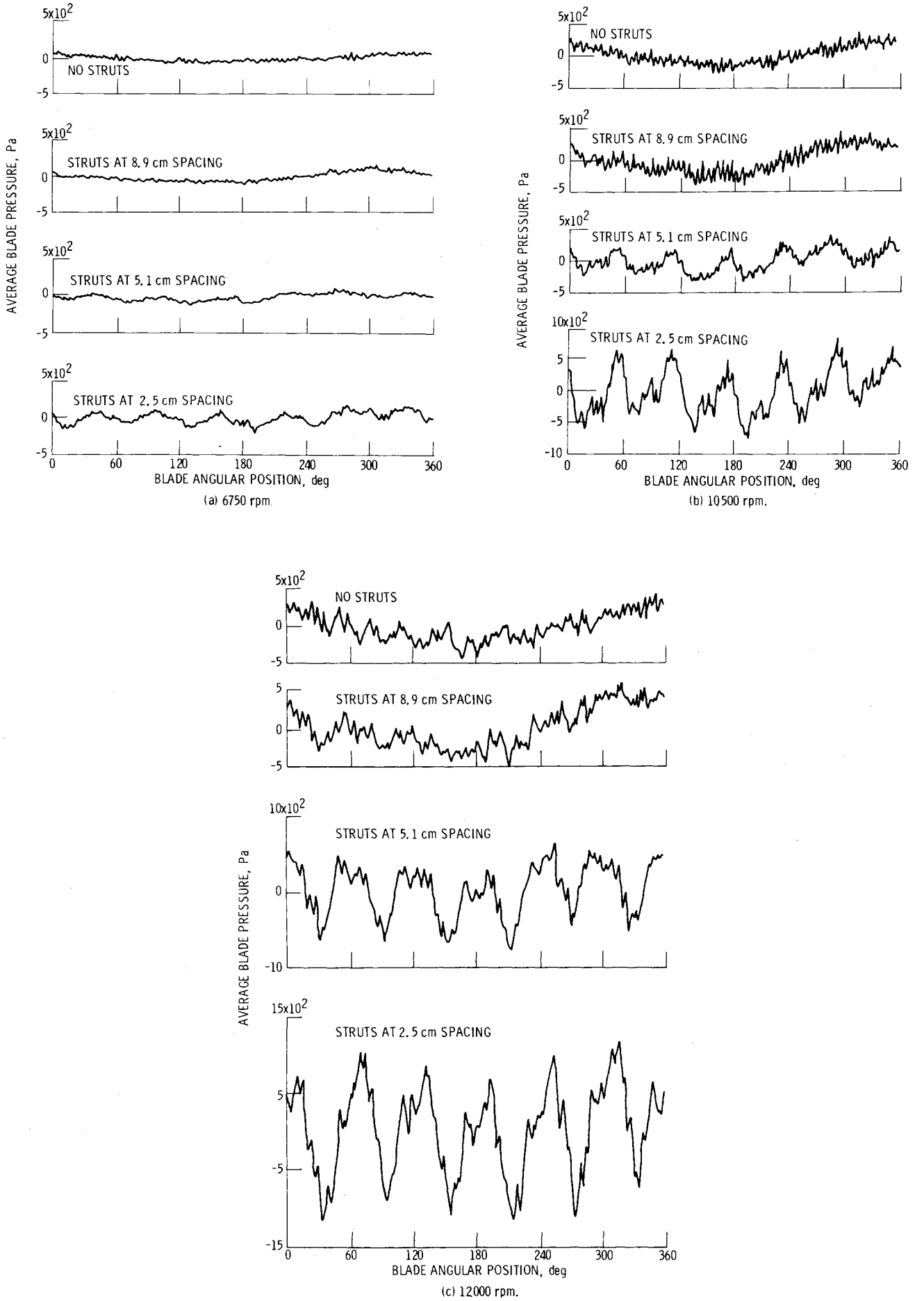

Fig. 12 Average blade pressure as a function of angular position (averaged over 500 revolutions, measured in direction of fan rotation from vertical top).

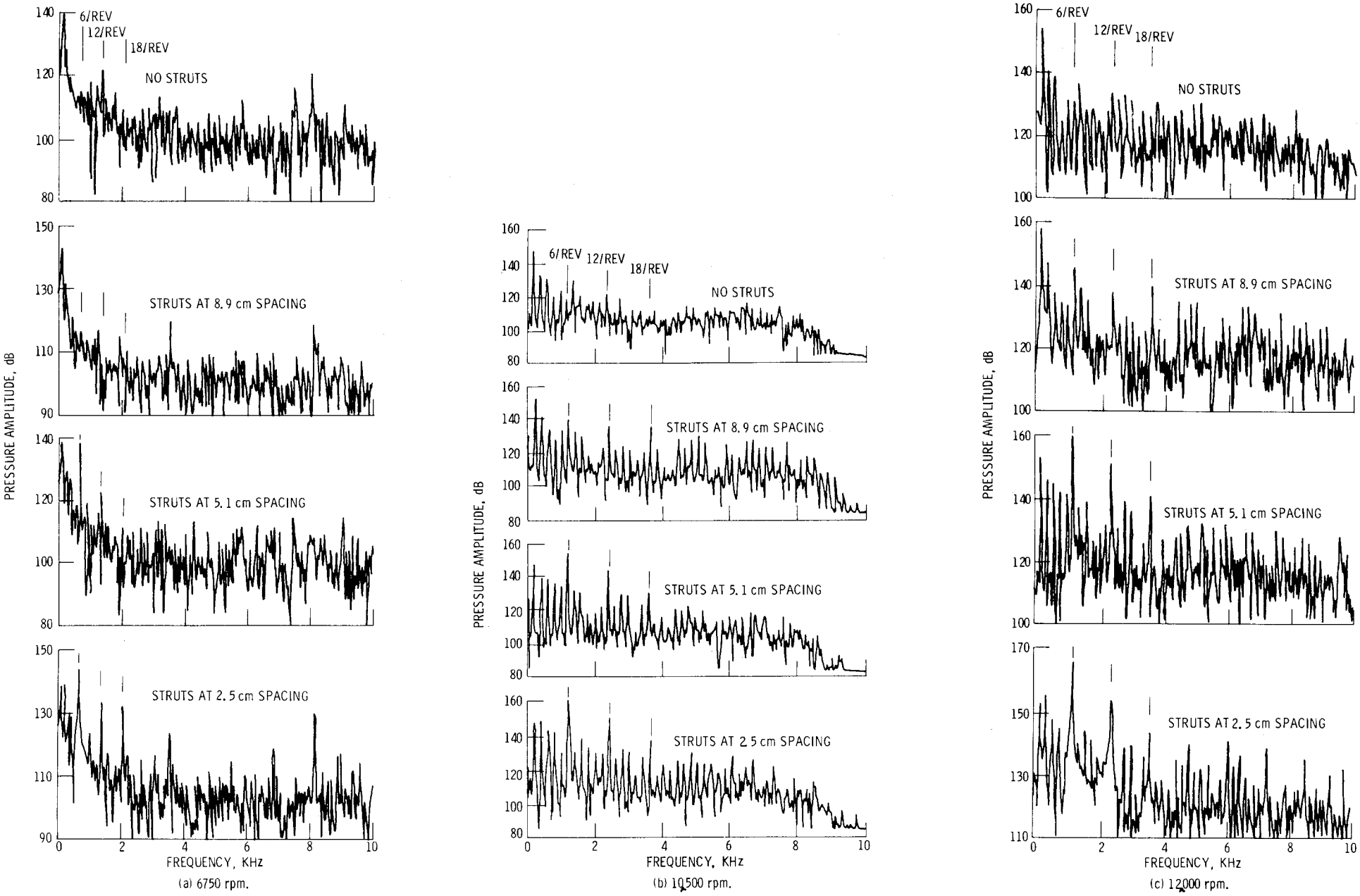

Fig. 13 Blade pressure amplitude spectra (pressure transducer B3).

Applying this expression to the fundamental tone for the rotor-strut interaction at 11, 300 rpm results in an angle range of $\psi_x = 39\text{-}56$ deg based on ξ values for the inlet throat and highlight. However, this angle range falls below the observed peak angle (64 deg) shown in Fig. 9b .

Reference 13 points out that Eq. (2), which assumes that the vector normal to the wave front is undeviated from inside the inlet to the far field, is probably incorrect. Previous data-theory comparisons using Eq. (2) were influenced by inlet lip thickness. The correct constraint is probably the condition that group velocity is undeviated from inside the duct to the far field. The peak angle expression in Ref. 12 for the condition of uniform flow everywhere satisfies the criterion of invarient group velocity and is:

$$\cos\psi_x = \sqrt{1-1/\xi^2}\sqrt{1-M_D^2}\Big/\sqrt{1-M_D^2(1-1/\xi^2)} \qquad (3)$$

This expression gives an angle range $\psi_x = 52\text{-}71$ deg for the fundamental strut interaction tone at 11, 300 rpm, which is in good agreement with the experimental results of Fig. 9.

Figure 10 shows the fundamental tone directivity for the closest (2.5 cm) strut spacing and the no-strut configurations at several fan speeds. In each case the range of the principal interaction lobe peak angle, as predicted by Eq. (3), is indicated by a horizontal band. At 6750 rpm (Fig. 10a) the $m = 22$ and $m = 16$ modes do not propagate. However, the (10, 1) mode is cut on, and corresponding to the rotor interaction with the third harmonic of strut flowfield distortion, is predicted to peak in the range from 41-52 deg. These angles are in reasonable agreement with the directivity data in Fig. 10a. The results for 10, 500 rpm (Fig. 10b) show good agreement with the prediction for the (22, 1) mode peak angle. Similar agreement is shown for the previously discussed 11, 300 rpm results repeated in Fig. 10c. Again, at 12,000 rpm, where the rotor relative airflow is approaching sonic, the angle prediction for the (22, 1) mode (Fig. 10d) is also supported by the data.

Figure 11 presents the first and second overtone directivities at 11,300 rpm. There is a small level increase at forward angles for the first overtone (Fig. 10a) at the closest strut spacing, but no significant strut effects on the second overtone directivity (Fig. 10b).

Blade Pressure Effects

The blade pressure transducer results for the fan tests also showed evidence of strut interaction. Figure 12 shows the average blade pressure at three fan speeds as functions of angular position for the three strut spacings and for the struts removed. At 6750 rpm (Fig. 12a) only the closest spacing (2.5 cm) shows a clear indication of the six-strut interaction. At 10,500 rpm (Fig. 12b) and 12,000 rpm (Fig. 12c) evidence of the strut interaction is clearly seen at the 5.1 cm engine strut spacing, as well as strong strut interaction effects at the closer spacing. The smaller magnitude disturbances superimposed on the data of Fig. 12 are due to rotor interaction with the 66 bypass stator vanes.

Figure 13 shows the blade pressure amplitude spectra corresponding to the average pressures in Fig. 12. At 6750 rpm (Fig. 13a) the fundamental strut interaction (6/rev.) and its overtones (12/rev. and 18/rev.) are clearly seen at the closest spacing. (2.5 cm). The fundamental and first overtone are also seen at the 5.1 cm strut spacing. At 10,500 and 12,000 rpm (Figs. 13b and 13c) there is evidence of the fundamental and the first and second overtones at all three strut spacings. As expected, with the struts removed there are no pronounced disturbances at the strut interaction frequencies.

As mentioned in the Introduction, Ref. 8 shows how the downstream strut potential field may induce vibration in an upstream rotor. Although this result shows that the rotor experiences the strut potential field and that, therefore, this interaction is a probable noise generating mechanism, it does not allow the conclusion that this is the only, or even the dominant, mechanism. The rotor wakes probably pass through the stator and these, interacting with the struts, are a potential generating mechanism. In this case, the sixth harmonics sensed by the rotor blade mounted transducer would be due to the resulting 22-lobed rotating sound field, rather than the 6-lobed stationary potential field of the stator. In any case, it is clear from these acoustic results that this rotor-strut interaction may appear as a major noise source which should be considered in quiet turbofan engine design.

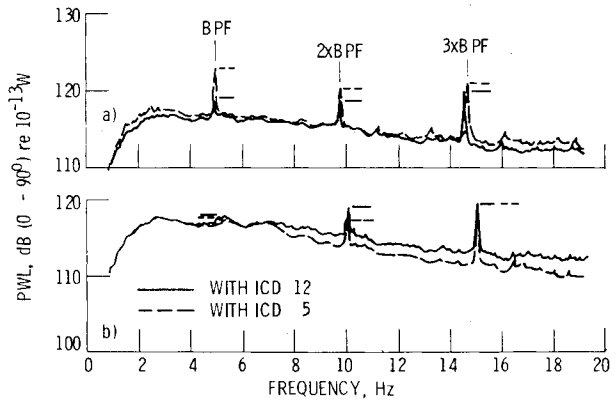

Fig. 14 Effect of B.L. suction on PWL spectra with support struts removed (10, 500 rpm).

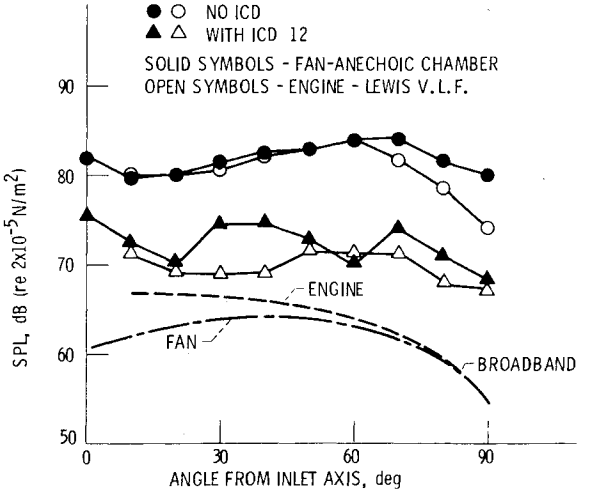

Fig. 15 Blade passage tone directivity (10, 500 corrected rpm, results adjusted for 30.5 m radius, 25 Hz bandwidth, fan struts at engine spacing).

Inflow Control

A major concern of the current study was to evaluate inflow control techniques for simulating flight acoustic performance to determine that the same structures were equally as effective in the anechoic chamber as in the outdoor engine stand. Acoustics tests were performed with the JT15D-1 engine flown on an aircraft, in simulated flight in the NASA Ames 40×80 foot Wind Tunnel, and statically with several inflow control devices. The JT15D fan was likewise tested with two ICD's, using the same hardware as was used for the Lewis static engine tests. In the anechoic chamber it was also possible to remove a portion of the inlet boundary layer upstream of the rotor (see Fig. 2) in an effort to identify noise associated with boundary layer disturbances or other disturbances near the wall.

Figure 14 compares the sound pressure level spectra obtained with the struts removed for ICD's 5 and 12 at 10, 500 rpm fan speed. With the hard duct configuration (Fig. 14a),

ICD 12 is shown to be somewhat more effective in reducing the BPT level. However, with the 10% boundary layer suction in the inlet duct (Fig. 14b), both ICD's are shown essentially to reduce the BPT level to that of the surrounding broadband. Thus it appears that a significant portion of the BPT level generated in static testing originates in the rotor tip region. ICD inlet mating considerations must be a critical element of the overall ICD design, since disturbances originating from this region would tend to enter the rotor in the tip region.

Comparison with JT15D-1 Engine

As was previously discussed, a basic goal of the current program was to validate inflow control structures on the JT15D fan/engine in several test enivironments. From prior engine tests conducted at Lewis, ICD 12 proved to be the most effective in reducing the blade passage tone levels among several ICD designs that were tested.[7] Figure 15 compares results for the Lewis static engine and fan tests, using ICD 12. The anechoic chamber data were corrected for distance and bandwidth to the engine measurement conditions. There is reasonably good agreement for the baseline and ICD 12 configurations between the engine and fan. The somewhat more lobed directivity for the fan with inflow control may be caused by the anechoic chamber installation with its greater possibility for wall-induced turbulence (see Fig. 2). Boundary layer suction essentially removes these lobes in the directivity results for the fan with ICD 12.

Summary

1) The previously identified interaction between the rotor and the six downstream support struts of the JT15D engine was further investigated through the testing of simulated support struts at three axial spacings. The JT15D fan stage installation in the anechoic chamber did not normally require downstream support struts, allowing the fan stage to also be tested with no struts. The $m = 22$ spinning mode generated by the rotor-strut interaction was evident in the acoustic directivity results, where the sound pressure level was increased by as much as 10 dB at the closest strut spacing. A theoretical prediction for lobe maximum intensity angle, based on invariance of the group velocity from duct to far field, showed good agreement with the data from these static tests.

2) The quality of the mating region between an ICD and the fan inlet appears to be very important to the overall performance of the ICD in reducing the fan BPT level. By removing residual inlet wall disturbances with boundary layer suction it was possible to further reduce the fan BPT level to that of the surrounding broadband when the support struts were also removed.

3) With the same inflow control device in place, reasonably good agreement was shown between results for the engine on the outdoor test stand and the fan in the anechoic chamber.

References

[1]Ho, P.Y., "The Effect of Vane-Frame Design on Rotor-Stator Interaction Noise," AIAA Paper 81-2034, Oct. 1981.

[2]Wazyniak, J.A., Shaw, L.M., and Essary, J.D., "Characteristics of an Anechoic Chamber for Fan Noise Testing," NASA TM X-73555, March 1977.

[3]McArdle, J.G., Jones, W.L., Heidelberg, L.J., and Homyak, L., "Comparison of Several Inflow Control Devices for Flight Simulation of Fan Tone Noise Using a JT15D-1 Engine," AIAA Paper 80-1025, June 1980.

[4]Schoenster, J.A., "Fluctuating Pressures on Fan Blades of a Turbofan Engine," NASA TP-1976, March 1982.

[5]Priesser, J.S., Schoenster, J.A., Golub, R.A., and Horne, C., "Unsteady Fan Blade Pressure and Acoustic Radiation from a JT15D-1 Turbofan Engine at Simulated Forward Speed," AIAA Paper 81-0096, Jan. 1981.

[6]Chestnutt, D., "Flight Effects of Fan Noise," NASA CP-2242, Sept. 1982.

[7]Homyak, L., McArdle, J.G., and Heidelberg, L.J., "A Compact Inflow Control Device for Simulating Flight Fan Noise," AIAA Paper 83-0680, April 1983.

[8]Yokoi, S., Nagano, S., and Kakehi, Y., "Reduction of Strut Induced Rotor Blade Vibration with the Modified Stator Setting Angles," *International Symposium on Airbreathing Engines,* 5th Ed., Bangalore, India, Feb. 1981, pp. 61-1 to 61-7.

[9]Kantola, R.A., and Warren, R.E., "Reduction of Rotor-Turbulence Interaction Noise in Static Fan Noise Testing," AIAA Paper 79-0656, March 1979.

[10]Englund, D.R., Grant, H.P., and Lanati, G.A., "Measuring Unsteady Pressure on Rotating Compressor Blades," NASA TM-79159, 1979.

[11]Heidmann, M.F., Saule, A.V., and McArdle, J.G., "Predicted and Observed Modal Radiation Patterns from JT15D Engine with Inlet Rods," *Journal of Aircraft,* Vol. 17, July 1980, pp. 493-499.

[12]Rice, E.J., Heidmann, M.F., and Sofrin, T.G., "Modal Propagation Angles in a Cylindrical Duct with Flow and Their Relation to Sound Radiation," AIAA Paper 79-0183, Jan. 1979.

[13]Groeneweg, J.F., and Rice, Edward J., "Aircraft Turbofan Noise," ASME Paper 83-GT-197, *28th ASME International Gas Turbine Conference,* Phoenix, Ariz., March 27-31, 1983.